

NJC

Accepted Manuscript



This is an *Accepted Manuscript*, which has been through the Royal Society of Chemistry peer review process and has been accepted for publication.

Accepted Manuscripts are published online shortly after acceptance, before technical editing, formatting and proof reading. Using this free service, authors can make their results available to the community, in citable form, before we publish the edited article. We will replace this *Accepted Manuscript* with the edited and formatted *Advance Article* as soon as it is available.

You can find more information about *Accepted Manuscripts* in the [Information for Authors](#).

Please note that technical editing may introduce minor changes to the text and/or graphics, which may alter content. The journal's standard [Terms & Conditions](#) and the [Ethical guidelines](#) still apply. In no event shall the Royal Society of Chemistry be held responsible for any errors or omissions in this *Accepted Manuscript* or any consequences arising from the use of any information it contains.

Revised 2**In situ thermal synthesis of novel polyimide nanocomposite films containing organo-modified layered double hydroxide: Morphological, thermal and mechanical properties**

Mohammad Dinari ^{*,1} Parvin Asadi,² and Solyman Khajeh³

¹*Department of Chemistry, Isfahan University of Technology, Isfahan, 84156-83111, I. R. Iran.*

²*Department of Medicinal Chemistry, School of Pharmacy and Pharmaceutical Sciences, Isfahan University of Medical Sciences, Isfahan, 81746-73461, I. R. Iran.*

³*Department of Chemistry, Payame Noor University, P.O. BOX 19395-4697, Tehran, I. R. Iran.*

* - Corresponding author. Tel.: +98 3133913270; fax: +98 3133912351.

E-mail address: dinari@cc.iut.ac.ir; mdinary@gmail.com

Abstract

An organic-inorganic hybrid compound constituted by a Zn/Al layered double hydroxide (LDH) intercalated with citric acid (LDH-CA), was dispersed in polyimides (PIs) with *N*-benzoxitrile side group, through *in situ* polymerization. At first, 3-(bis(4-aminophenyl)amino)benzoxitrile as a diamine monomer was synthesis and then it was reacted with 4,4'-benzophenone tetracarboxylic dianhydride via thermal imidization method to formed processable PI. To improve the thermal and mechanical properties and also to avoid the aggregation of LDH particle in the polymer matrix, small amount of LDH-CA (1, 2, 4 wt %) was added to the synthesized PI. The resulted materials were characterized by Fourier transform-infrared spectroscopy, X-ray powder diffraction, thermogravimetry analysis (TGA), field emission-scanning electron microscopy, and transmission electron microscopy (TEM) techniques. TEM results showed that the LDH-CA nanolayers were dispersed in PI matrixes. The mechanical and thermal properties of the synthesized composites are effectively enhanced by the incorporation of 2wt.% LDH-CA in the polymer matrix. For the PI/LDH-CA nanocomposites, the maximum degree of tensile strength is observed at a LDH-CA loading of 2 wt%, corresponding to an almost 32% increase in tensile strength compared to the pure PI.

Keywords: ZnAl-layered double hydroxide; polyimides; *in situ* polymerization; Tensile strength; Thermal properties

Introduction

Organic/inorganic hybrid materials have attracted widespread consideration owing to their potential uses as flame retardant materials, gene and drug delivery and catalyst carriers.¹ Polymeric nanocomposites (NCs) are a new class of materials consisting of nanosized fillers in a polymeric matrix, and possess properties superior to those of conventional microsized filler composites, due to the ultrafine dimensions of the filler.^{2,3} Moreover, on account of the unique properties such as enhanced mechanical and thermal properties, reduced flammability as well as high chemical stability, polymer/layered crystal NCs have been recognized as one of the most important organic/inorganic hybrid materials.⁴⁻⁶ Most of the published works has focused on organically modified smectite clays, in particular montmorillonites, as fillers of polymeric composites.⁷⁻⁹ Furthermore, the emphasis is placed on layered double hydroxide (LDH) systems rather than clays in recent years due to artificially preparing and highly tunable properties.^{10,11} LDHs are a kind of anion clay with unique properties that are not commonly observed in layered silicates. LDHs are well characterized and conventionally used for flame retardants,¹² catalysts,¹³ ion exchangers,¹⁴ matrices for biosensors,¹⁵ and supercapacitor electrode material.¹⁶ Their novelty originate from their broad range of chemical composition, highly tunable properties, ease of synthetic procedures in the laboratory, stability in air, interchangeable anions and their potential industrial uses.¹⁷ Ultrathin nanosheets, prepared by delamination of layered hydroxides, have attracted attention due to the extremely small thickness of the order of 1 nm and large lateral size of the order of micrometers.¹⁸ Chemical composition of LDHs can be represented by the generic formula $[M^{2+}_{1-x} M^{3+}_x(OH)_2][(A^{n-})_{x/n} \cdot mH_2O]$.^{17,18} Common features of these compounds are positively charged 'host' layers of mixed metal (M^{2+} and M^{3+}) hydroxide, charge-compensating layers of 'guest' anions, and water molecules in interstitial positions.¹⁹

However, the surface characteristic of LDH is hydrophilic and it is difficult to realize the intercalation of polymer into the interlayers because of the integrated hydrogen-bonding network between the hydroxide layers, intercalated anions and water molecules. When certain organic anions are present in the interlayer space, the surface of LDHs can be rendered from hydrophilic to hydrophobic and as a result may be used to prepare polymer/LDH NCs. To make the more compatible LDH with most hydrophobic polymers, the appropriate interlamellar surface modification of LDH is essential for the preparation of LDH based polymer NCs.^{3,20-22} Organically modified LDH have been dispersed in various polymers, such as polypropylene,²³ polystyrene,²⁴ poly (methyl methacrylate),²⁵ polylactide,²⁶ polyimide (PI),²⁷ poly(amide-imide)²⁸ and poly(ethylene glycol diacrylate).²⁹ Because of their highly tunable properties, these NC materials are evaluated for potential application in a large number of fields, such as those emphasizing mechanical performance and as polymer electrolytes.³⁰

Thermally stable organic polymers have been the subject of various studies to enlarge the application of organic materials in harsh environment.³¹ Of thermally stable organic polymers, the excellent properties of aromatic PIs such as outstanding thermooxidative stability and higher chemical resistance led to the use of PIs in different area, such as insulating materials for electronics, semipermeable membranes for gas separation, and high-temperature adhesives and coatings.^{32,33} In spite of their excellent properties, aromatic PIs have a few problems in which inefficient processability is most obvious one originating from their very high glass-transition temperature and lack of efficient solubility in common organic solvents.³⁴ Therefore, extensive efforts such as introducing of bulky pendent groups, flexible linkage, noncoplanar structures and or copolymerizing from different diamines or dianhydrides have been made to improve their processability.³⁵⁻³⁸ With these modification methods, the melting temperatures can be

significantly lowered, and the solubility may be much improved, which results in processable PIs.³⁴

The extent of improvement in the NC properties depends on the state of dispersion of the silicate layers of the organoclay. Apart from the chemical structure and the length of the organic moiety in the organoclay, the processing conditions determine the state of dispersion. Several approaches were examined by Delozier et al. for PI-clay NCs.² According to their findings, the best results were obtained using an in situ polymerization technique, wherein polyamic acid (PAA) was synthesized in the presence of organoclay, and then it was thermally imidized using a solution-casting technique. In the present work, a soluble aromatic PI containing pendant benzonitrile groups was synthesized by the reaction of 3-(bis(4-aminophenyl)amino)benzonitrile and 4,4'-benzophenone tetracarboxylic dianhydride (BTDA) by thermal imidization method. Then, we report the synthesis, characterization and properties of partially exfoliated NCs by in situ polymerization technique under thermal imidization method. In order to make a homogeneous dispersion in the polymer matrix, the inorganic LDH was made organophilic by the intercalation of citric acid (LDH-CA) anion in the interlayer. Characterization focused on the morphology, mechanical and thermal properties of the novel hybrid materials.

Experimental

Materials

All materials and solvents were purchased from Merck Chemical Co and Aldrich Chemical CO. 3-Aminobenzonitrile, 1-fluoro-4-nitrobenzene, BTDA, palladium on activated carbon (10 wt%) and hydrazine hydrates were used as received. *N*-methyl-2-pyrrolidone (NMP), *N,N*-dimethylformamide (DMF) and *N,N'*-dimethylacetamide (DMAc) were dried over barium oxide,

followed by fractional distillation. Citric acid ($\geq 99.5\%$, $M_w=192.12$ g/mol), Zinc nitrate hexahydrate $[\text{Zn}(\text{NO}_3)_2 \cdot 6\text{H}_2\text{O}]$, Aluminum nitrate nonahydrate $[\text{Al}(\text{NO}_3)_3 \cdot 9\text{H}_2\text{O}]$ and sodium hydroxide (NaOH) were used as received. Deionized water was used throughout the experiments.

Synthesis of diamine monomer

Diamine monomer was synthesis in two steps. At first, 3-(bis(4-nitrophenyl)amino)benzotrile was prepared by nucleophilic substitution reaction of 3-aminobenzotrile with 1-fluoro-4-nitrobenzene in the presence of cesium fluoride in DMSO; yield = 90%, melting point= 218-220 °C. In the second step, the nitro groups were reduced to the corresponding amines with hydrazine hydrate as the reducing agent and palladium as the catalyst as shown in Scheme 1. The purity of this monomer was checked by thin layer chromatography, which showed one spot in an ethylacetate/cyclohexane mixture (50:50) with $R_f = 0.42$. The yield was 81%; melting point= 188- 191 °C.³⁷

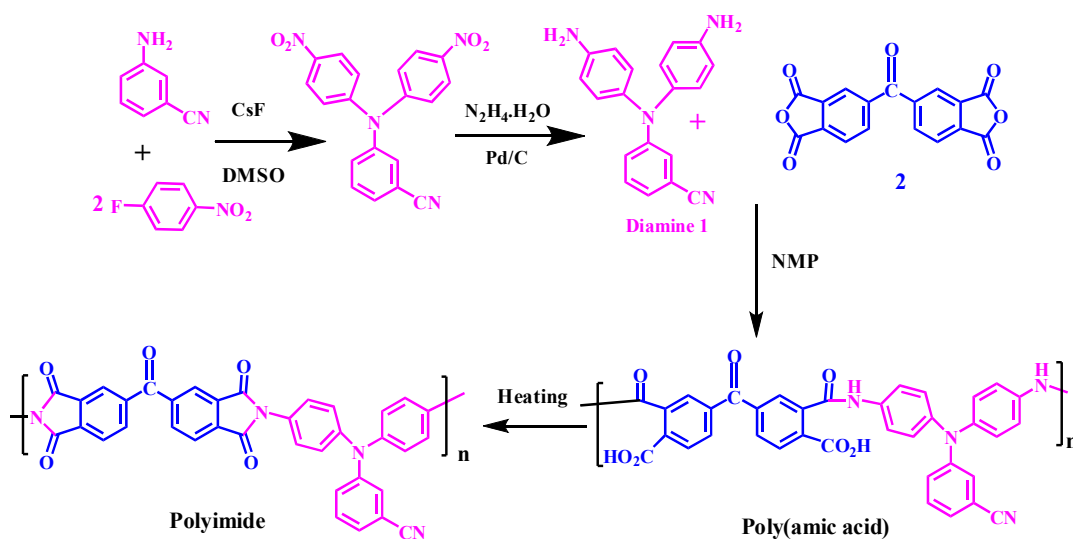
FTIR (KBr, cm^{-1}) of diamine 1: 3448 (s), 3377 (s), 3113 (w), 3075 (w), 2225 (s), 1555 (m), 1440 (w), 1323 (w), 1252 (w), 844 (m), 739 (w). ¹H-NMR (400 MHz, DMSO- d_6 , ppm) of diamine 2: 4.49 (s, 4H, NH), 6.26-6.28 (d, 8H, Ar-H, $J = 4.5$ Hz), 6.49 (s, 1H, Ar-H), 6.76-6.78 (d, 1H, Ar-H), 7.19-7.20 (d, 1H, Ar-H, $J = 4$ Hz), 7.36-7.38 (dd, 1H, Ar-H, $J = 4$ Hz).

Preparation of polyamic acid (PAA) and pristine PI

2.00 g (6.66 mmol) of 3-(bis(4-aminophenyl)amino)benzotrile as diamine monomer 1 was dissolved in NMP (20 wt%) and cooled with the ice water bath. After completely dissolved, BTDA (2.15 g, 6.66 mmol) as the anhydride monomer 2 was added into the above solution under stirring with a mechanical stirrer, a condenser and a nitrogen inlet for 6 h at room temperature to obtain the pristine PAA. The inherent viscosity of the PAA was 0.97 dL/g, as measured in

DMAc at a concentration of 0.5 g/dL at 30 °C. The PAA was converted into PI with a thermal imidization method. In this method, about 1.00 g of the PAA solution was spread into a Petri dish 7 cm in diameter and baked at 90 °C overnight (ca. 12 h) for the removal of the casting solvent. The semidried PAA film was further dried and converted into the PI by sequential heating at 150 °C for 1 h, at 200 °C for 1 h, and at 300 °C for 3 h. To ensure the completion of imidization, the PI films were further heated at 350 °C for another 1 h. and then were examined by elemental analysis, tensile testing, X-ray crystallography, and thermal analysis.

PI: FTIR (KBr, cm^{-1}): 3106 (aromatic C-H stretching), 2217 (stretching $\text{C}\equiv\text{N}$), 1777 (asymmetric imide $\text{C}=\text{O}$ stretching), 1726 (symmetric imide $\text{C}=\text{O}$ stretching), 1629 (aromatic $\text{C}=\text{C}$ stretching), 825 (C-N bending). $^1\text{H-NMR}$ (400 MHz, DMSO-d_6 , ppm): 6.15-6.16 (d, 2H, Ar-H, $J= 3.5$), 6.55 (s, 2H, Ar-H, $J= 4.5$ Hz), 6.62-7.64 (d, 2H, Ar-H, $J= 4.5$ Hz), 6.71 (s, 1H, Ar-H), 7.45-7.46 (d, 1H, Ar-H, $J= 3.5$), 7.53-7.55 (d, 1H, Ar-H, $J= 3.5$), 7.78-7.80 (d, 1H, Ar-H, $J= 4.5$ Hz), 7.82-7.83 (d, 1H, Ar-H, $J= 3.5$), 8.17-8.19 (d, 1H, Ar-H, $J= 4.5$ Hz), 8.26-8.28 (d, 1H, Ar-H, $J= 4.5$ Hz), 8.46-8.48 (d, 1H, Ar-H, $J= 4.5$ Hz). Anal. Calcd. for $\text{C}_{36}\text{H}_{18}\text{N}_4\text{O}_5$ (586.55 g/mol): C, 73.72%; H, 3.09%; N, 9.55%. Found: C, 73.77%; H, 3.13%; N, 9.48%.



Scheme 1. Synthesis of diamine, PAA and PI.

Synthesis of CA modified Zn/Al LDH (LDH-CA)

Citric acid (CA) with one hydroxyl and three carboxyl groups exist widely in citrus fruits and pineapples. The LDH-CA was prepared using co-precipitation technique as shown in Fig. 1: a mixed metal solution of $\text{Zn}(\text{NO}_3)_2 \cdot 6\text{H}_2\text{O}$ (4.6 g, 0.015 mol) and $\text{Al}(\text{NO}_3)_3 \cdot 9\text{H}_2\text{O}$ (1.8 g, 0.030 mol) with 2:1 molar ratio in 100 mL decarbonated water was added dropwisely over 2 h to an aqueous solution containing 0.015 mol of CA under nitrogen atmosphere with vigorous stirring. During the titration, the solution pH was adjusted to 7-8 with 0.1 N NaOH solutions to induce co-precipitation reaction. The mixture was sonicated with a frequency of 2.25×10^4 Hz and power of 100W for 2h under nitrogen atmosphere. Finally, the obtained suspension was filtrated using Whatman filter paper and washed four times by dispersion in distilled water and filtration and it was dried at 60 °C for 12 h. For comparative study, Zn/Al LDH- CO_3^{2-} was prepared under identical reaction conditions without using CA compound.

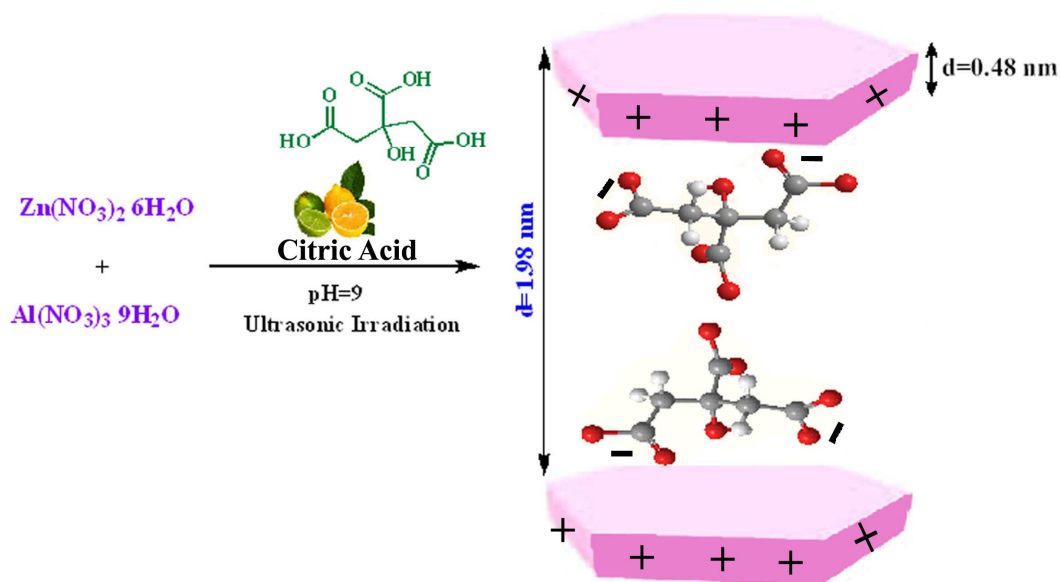
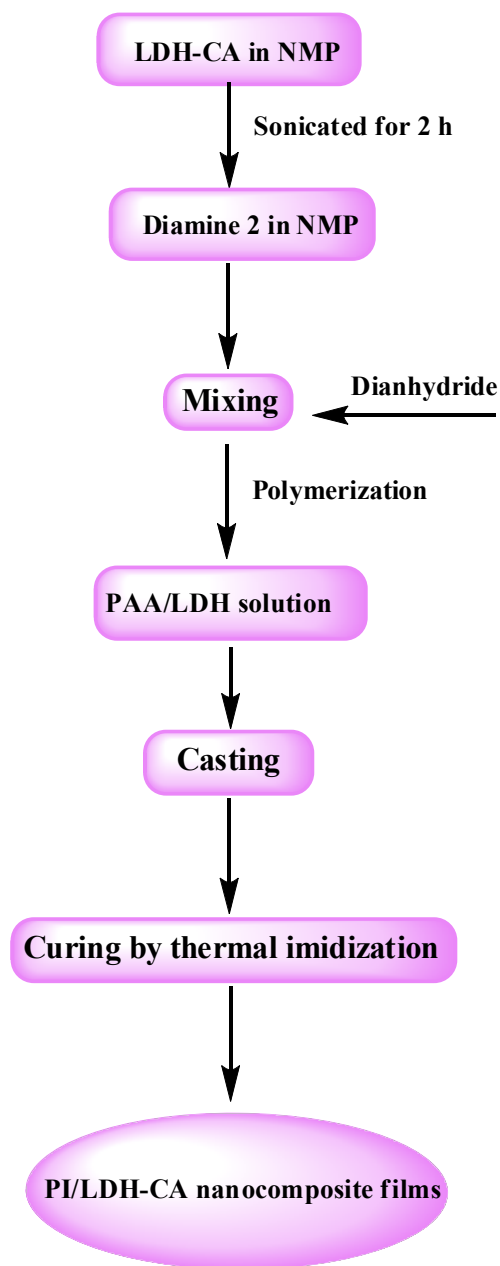


Fig. 1. Preparation of citrate intercalated LDH (LDH-CA).

Preparation of PI/LDH-CA NC films

Various contents of LDH-CA (1, 2 and 4 wt%), were dispersed in NMP (5 mL) under sonication for 2 h in order to prepare various concentrations of LDH-CA nanoparticles. Diamine (0.5 g, 1.5 mmol) was added to flasks containing various concentrations of the LDH-CA in NMP solution under a nitrogen purge in a sonic bath. After diamine was completely dissolved in the LDH-CA/NMP solutions, 0.54 g (1.5 mmol) of BTDA was added, and then the mixtures were stirred at room temperature under a nitrogen purge. The solid concentration of the solutions was kept at 10 wt% for all of the compositions. After 12 h, viscous PAA/LDH-CA solutions were obtained. These PAA precursor solutions were cast onto clean, dry glass substrates. The as-cast films were soft-baked at 80 °C for 12 h and then thermally imidized using a stepwise imidization process under a nitrogen atmosphere for 1 h at 150 and 200 °C, and 3 h at 300 °C. The overall process is summarized by the flow charts in Scheme 2. The average thickness of the composite films varied from 6 to 30 μm. All of the films were stored in desiccators prior to their characterization.



Scheme 2. Flow charts diagram for the preparation of PI/LDH-CA NC films.

Techniques

Fourier transform-infrared (FT-IR) spectra of the samples were recorded at room temperature in the range of 4000-400 cm^{-1} at a resolution of 4 cm^{-1} , on (Jasco-680, Japan) spectrophotometer. Spectra of solids were obtained using KBr pellets. Vibrational transition frequencies are reported in wavenumber (cm^{-1}). The band intensities are assigned as weak (w), medium (m), shoulder

(sh), strong (s), and broad (br). Inherent viscosities (η_{inh}) were measured by a standard procedure using a Cannon-Fenske Routine Viscometer (Germany) at 30 ± 0.5 °C. Nuclear magnetic resonance (NMR) spectra were recorded on a Bruker Avance DRX 400 and 100 MHz, by using solutions in deuterated dimethylsulfoxide (DMSO- d_6). The Proton resonances were designated as singlet (s) and multiplet (m). Carbon, hydrogen and nitrogen content of the compounds were determined by pyrolysis method by Vario EL elemental analyzer. X-ray diffraction (XRD) patterns were recorded using CuK_{α} radiation on a Bruker (Germany), D8Avance, diffractometer operating at current of 100 mA and a voltage of 45 kV. The diffractograms were measured for 2θ , in the range of $1.2-80^{\circ}$, using CuK_{α} incident beam ($\lambda = 1.51418$ Å). And Bragg's law $n\lambda = 2d\sin\theta$ was used to compute the d-spacing. Thermal stability was measured with a thermogravimetry analysis (TGA) (TA instrument Co.) at a heating rate of 20 °C min^{-1} from room temperature to 800 °C under a continuous flow of nitrogen. The morphology of the hybrid materials was examined by field emission-scanning electron microscopy [(FE-SEM), HITACHI; S-4160]. The powdered sample was dispersed in H_2O , and then the sediment was dried at room temperature before gold coating. Transmission electron microscopy (TEM) images were recorded using a Philips CM120 (Eindhoven, Netherland) with an accelerator voltage of 100 kV. The NC films were first microtomed into 60 nm ultra thin sections with a diamond knife using Leica Ultracut UCT ultramicrotome. Tensile strength and elongation at break of the NC films were measured with the help of UTM-INSTRON, PLUS, Model No. 8800. Test samples with dimension of 10×25 mm² and thickness in the range of 6 to 30 μm were used for the measurement of tensile strength and percentage of elongation at break.

Results and discussion

FT-IR and ¹H-NMR study

FT-IR, ¹H-NMR and elemental analysis data of the diamine monomer 1 are reported in the experimental section. In the FT-IR spectrum of the diamine, the characteristic absorptions of the nitrile groups were observed at 2225 cm⁻¹. The characteristic absorptions of the amine group showed the typical N-H stretching absorption pair in the region of 3448-3377 cm⁻¹. In the ¹H-NMR spectrum of the diamine compound 1, a peak at 4.50 ppm was assigned to the amine protons group and all aromatic protons appeared at 6.2-7.4 ppm. The FT-IR and NMR spectra of the diamine 1 was reported in our previous articles.³⁷

Conversion of the PAA to the fully cyclized PI was proved by means of by FT-IR, ¹H NMR spectroscopy and elemental analysis techniques. The FT-IR spectra of the PAA and corresponding PI based on BTDA are presented in Fig. 2. As shown in Fig. 2a, PAA showed a broad absorption characteristic band of carboxylic O-H and amide N-H groups at about 2600-3700 cm⁻¹ and a narrow characteristic band at 1685 cm⁻¹ associated to C=O of amide linkage. After thermal imidization, these peaks were disappeared. In the spectra of the PI, absorption bands of the imide groups appear at 1777 and 1726 cm⁻¹ for the symmetric and anti-symmetric stretching vibrations of the carbonyl groups.³⁸ Other characteristic absorption bands of the imide were appeared at 1356 and 825 cm⁻¹ for the C-N stretching and C=O bending, respectively (Fig. 2b). In the ¹H-NMR spectrum of the PI, all the peaks have been readily assigned to the hydrogen atoms of the repeating unit and no amide or acid protons at 10-13 ppm were appeared. This indicating that complete imidization was really achieved. Good agreement between calculated and found amounts of C, H, and N content was observed in elemental analysis of PI approving its proposed structure.

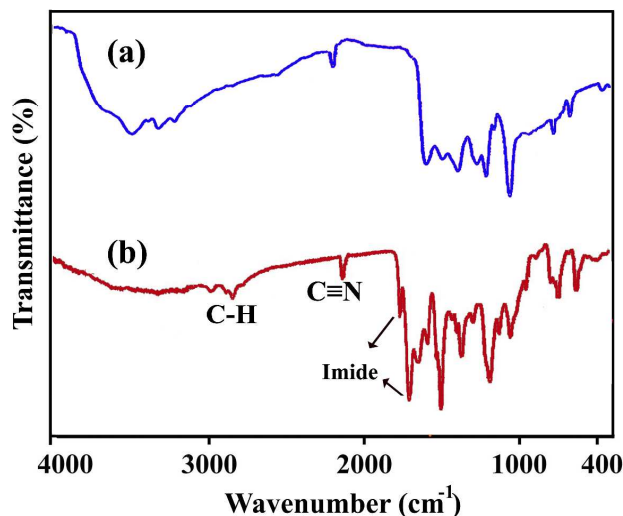


Fig. 2. FT-IR spectra of the PAA (a) and neat PI (b).

Fig. 3 shows the FT-IR spectra of the LDH-CA and PI NCs with 1, 2, 4 wt.% of LDH-CA. A broad absorption peak between 3600 and 3000 cm^{-1} is assigned to O-H group stretches of both the hydroxide layers and the interlayer water (Fig. 3a).³⁹ Weaker bands arising from aliphatic C-H stretches is observed in the range of 2950-2850 cm^{-1} . The asymmetric and symmetric carboxylated anion of the CA was observed at around 1582 and 1398 cm^{-1} , respectively.^{39,40} The bands around 780, 554 and 440-450 cm^{-1} are caused by various lattice vibrations associated with metal hydroxide sheets.^{14,39} Figs. 3b-3e shows the FT-IR spectra of the neat PI and PI NCs with different amount of LDH-CA. A broad absorption between 3600 and 3200 cm^{-1} was associated with the stretching mode of hydrogen-bonded hydroxy groups from both the hydroxide layers and interlayer water in LDH-CA. In the FT-IR spectra of the NC with different amount of LDH-CA, the symmetric and anti-symmetric stretching vibrations of the carbonyl groups of the imide shifted from 1777 and 1726 cm^{-1} to 1772 and 1721 cm^{-1} , respectively, in comparison with neat PI. Also, in addition to the PI peaks, the FT-IR spectra of the PI/LDH-CA NCs show new absorption bands at 700-400 cm^{-1} for metal hydroxide sheets.⁴¹

This result verifies that LDH-CA was successfully formed in the hybrid PI composites by the thermal imidization techniques (Fig. 3c-3e).

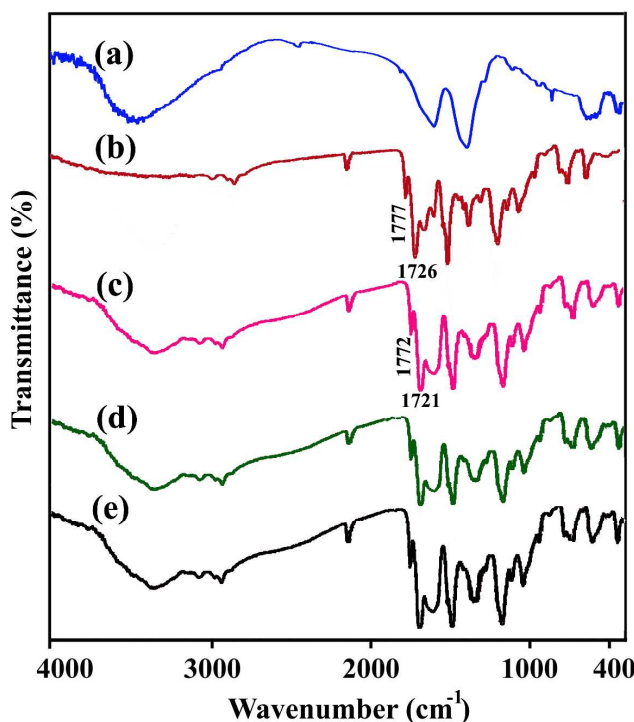


Fig. 3. FT-IR spectra of LDH-CA (a), neat PI (b) and NC with 1 (b), 2 (c) and 4wt.% (e) of LDH-CA.

X-ray diffraction

XRD patterns of the ZnAl-CO₃²⁻ LDH and LDH-CA are shown in Fig. 4. The XRD patterns of the ZnAl-CO₃²⁻ compounds display the characteristic reflections of LDH with the basal peaks for (003) and (006) planes at low 2θ angle and the nonbasal peaks for (101), (015), (018), (110) and (113) planes at high 2θ angle.⁴² For ZnAl-CO₃²⁻ LDH, the interlayer d spacing of characteristic (003) planes (d_{003}) at $2\theta = 11.42^\circ$ was found to be 0.76 nm which is similar to the values reported previously,^{43,44} indicating that Zn/Al-LDH is well crystallized (Fig. 4a). As expected, the position of the basal reflections of LDH-CA is shifted to higher d value indicating the expansion in the interlayer distance (Fig. 4b). The XRD patterns of the LDH-CA showed the expanding

LDH structure with a sharp (003) spacing of 1.98 nm at $2\theta = 4.38^\circ$. Given that the thickness of the brucite-like layer of LDH is 0.48 nm,^{41,45} the gallery height in the LDH-CA is 0.71 nm, compared with 0.28 nm in the carbonate-containing LDH. These data suggest a monolayer arrangement for the intercalated carboxylate oriented perpendicular to the LDH layers. This finding reveals that citrate anions had intercalated into the gallery of the LDH layers (Fig. 1). XRD curves of neat PI and PI/LDH-CA films are also shown in Fig. 4c-4f. The PI/LDH-CA films do not show any diffraction peak in the range $2\theta = 1.2-10^\circ$ as opposed to the diffraction peak at $2\theta = 4.38^\circ$ for LDH-CA. Usually, there are two types of NCs depending upon the dispersion of clay particles.²⁷ The first type is an intercalated polymer/clay NCs, which consists of well-ordered multilayers of polymer. In these NC samples, the extent of polymer penetration is not sufficient to delaminate the ordered structures. The second type is an exfoliated polymer/clay NCs, in which there is a loss of ordered structure due to the extensive penetration of polymer into the silicate layers.⁴⁶ In the case of the PI/LDH-CA hybrid films, the XRD curves indicate the possibility of exfoliated silicate layers of LDH-CA being dispersed in PI. XRD curves of the PI/LDH-CA films are shown in Fig. 4. No peaks appear when the LDH-CA contents are 1, 2 and 4 wt%. This indicates the exfoliated silicate layers of LDH-CA might be dispersed in PI. While XRD provides a partial picture about distribution of nanofiller and disappearance of peak corresponding to d-spacing does not always confirm the exfoliated NCs, characterization of NC morphology need microscopic investigation. The complete disappearance of LDH peaks in the NC samples may be owing to the partial exfoliated structure, in which the gallery height of intercalated layers is large enough and the layer correlation is not detected by XRD.

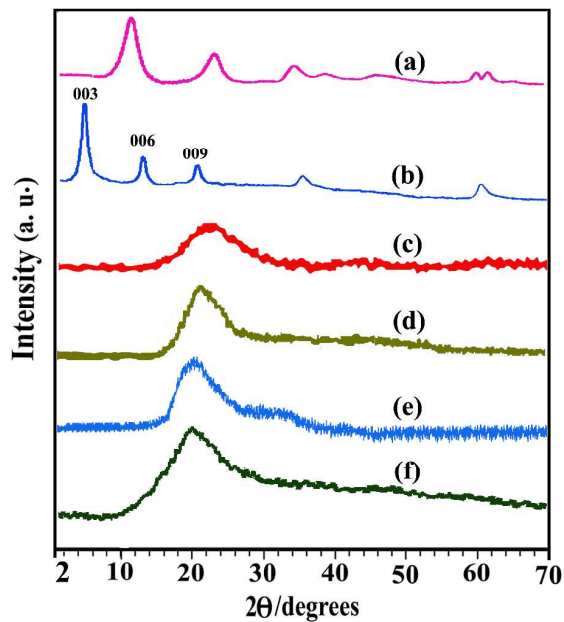


Fig. 4. XRD patterns of LDH-CO₃²⁻ (a), LDH-CA (b), NC with 1 (c), 2 (d) and 4wt.% (e) of LDH-CA and neat PI (f).

Morphology of PI/LDH-CA NCs

The FE-SEM and TEM images of the LDH-CA are presented in Fig. 5. According to these images, the particles exhibit typical hexagonal plate-like morphology, without curved or contorted sheets found (Fig. 5). It is clear, therefore, that the expanded basal spacing and reduced interaction between LDH layers due to CA anion intercalation facilitate the curved growth of LDH crystals along vesicle interfaces.

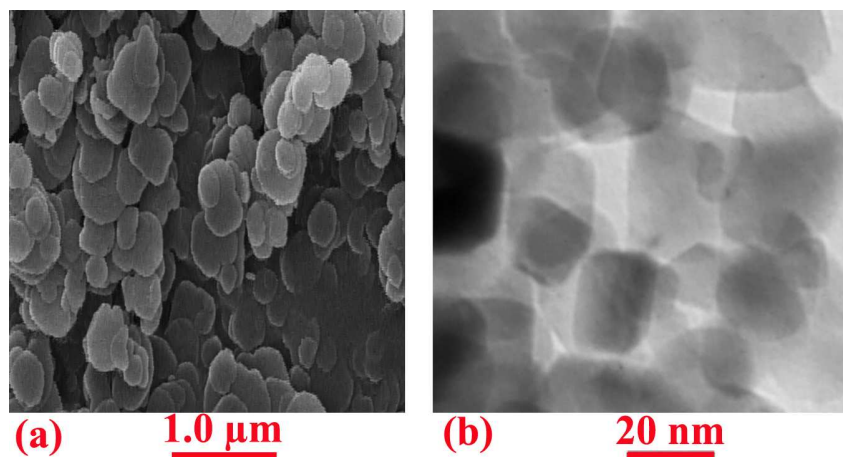


Fig. 5. FE-SEM (a) and TEM (b) images of LDH-CA.

FE-SEM and TEM images of NC materials with 2 and 4 wt.% of LDH-CA are shown in Fig. 6. In the FE-SEM images of the NC films with 2 and 4 wt.% of LDH-CA, the plate like structures of LDH was changed (Fig. 6a and 6c). Apparently, it seems that the particles are dispersed in the polymer matrix. In the NC with high LDH concentration, some aggregation may be observed in the FE-SEM pictures. For PI NC with 2 and 4 wt.% of LDH-CA, the TEM images reveal a coexistence of LDH-CA layers in the exfoliated states (Fig. 6b, 6d). Particles seem to be loose and not agglomerated was observed in the sample prepared by in situ polymerization, suggesting that this method may be suitable for dispersion of the inorganic filler in the polymer matrix (Fig. 6b). A little aggregations were observed in the TEM image of the PI/LDH-CA NC4% in comparison with NC2%. As a result, increasing the LDH-CA content leads to poor properties of the PI/LDH-CA NCs, because of the aggregation domains of the LDH-CA nanolayers.

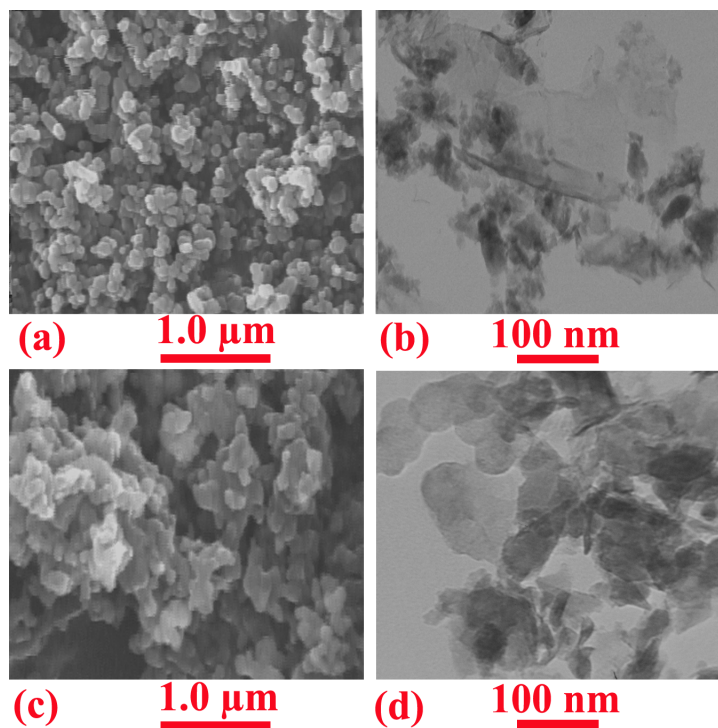


Fig. 6. FE-SEM (a, c) and TEM (b, d) images of NCs with 2 and 4% of LDH-CA.

Mechanical properties of PI/LDH-CA NC films

It is generally believed that external stress on a polymer composite is transferred from the continuous phase (polymer matrix) to the discontinuous phase (filler). Therefore, the ultimate properties of the composites are dependent on the extent of bonding between the two phases, the surface area of the nanofiller, and the arrangements between the filler particles.⁴⁷ Previous studies demonstrated that, the strength should be reduced if there are no bonding sites between the organic polymer phase and the inorganic nanofiller phase due to the inert nature of the PIs and the weak interactions between these polymers and the fillers.^{38,48,49} The tensile properties of the PI/LDH-CA NC films in terms of the increased degree of tensile strength relative to pure PI as function of LDH-CA content were examined by tensile testing and their stress–strain curves were shown in Fig. 7. The tensile strength at break was observed to increase with the LDH-CA

content. With 2 wt% LDH-CA content, the maximum tensile strength of the PI/LDH-CA NCs was 136 MPa, which is 32% higher than pure PI. In this study, citrate anion in LDH-CA, is the connection between the Zn/Al nanolayers and the PI matrix, increasing the compatibility between these two phases. Thus, the well dispersed Zn/Al nanolayers effectively enhance the tensile strength of the PI/LDH-CA NCs. Further additions of LDH-CA (4 wt%) don't enhance the strength because of increasing brittleness, as a few amount of Mg/Al nanolayers were aggregated to form a defect in the NCs, reducing tensile strength.⁴⁵ Interestingly, the elongation of the PI/LDH-CA NC films increased with LDH-CA content. With 2 wt.% LDH-CA content, the elongation at break was increased in comparison to the pure PI. By the same reasoning, the elongation behavior of the PI/LDH-CA NCs is also determined by the interfacial bonding between the Zn/Al nanolayers and the PI matrix. When the LDH-CA content was increase to 4 wt.%, the strain was reduced which is confirm that some aggregation of the Zn/Al nanolayers was occurred.

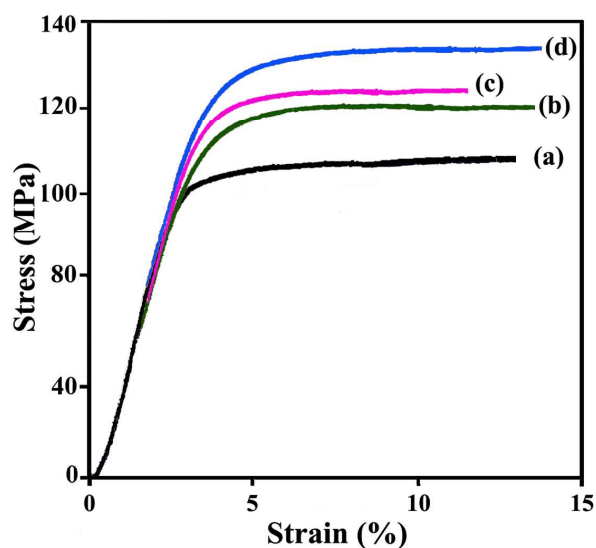


Fig. 7. Tensile stress-strain curves of neat PI (a), and NC with 1 (b), 4 (c) and 2wt.% (d) of LDH-CA.

Thermal properties

The thermal stability of the pure polymer and PI/LDH-CA NCs was evaluated by TGA experiments at $20\text{ }^{\circ}\text{C min}^{-1}$ from 20 to $800\text{ }^{\circ}\text{C}$ as shown in Fig. 8. From Table 1, for all PI/LDH-CA NCs, an improvement in the onset temperature and in the midpoint temperature is observed. Pure PI film is quite stable up to $390\text{ }^{\circ}\text{C}$. The weight of the pure PI film remained around 98% under $400\text{ }^{\circ}\text{C}$, and then substantially decreased from $410\text{ }^{\circ}\text{C}$ to $550\text{ }^{\circ}\text{C}$. The PI/LDH-CA NC film showed a similar pattern of weight loss but at higher temperature than the pure PI films. The decomposition temperature at 5% ($T_{5\%}$) weight loss for these composites increases with the LDH-CA nanofillers loading. About $50\text{ }^{\circ}\text{C}$ improvements in $T_{5\%}$ is found in 2 wt% LDH-CA nanofillers loading. The 10 % weight loss temperatures ($T_{10\%}$) of the PI is $407\text{ }^{\circ}\text{C}$ and for NC materials with 1, 2 and 4wt% of LDH-CA, it is 436, 461 and $486\text{ }^{\circ}\text{C}$, respectively (Table 1). The char yields at $800\text{ }^{\circ}\text{C}$ of the NCs with different LDH-CA content are higher than that of pure PI. The char yield of NCs was from 70 to 74% at $800\text{ }^{\circ}\text{C}$. In reality the presence of the hydrotalcite-like lamellae produces a barrier to oxygen diffusion into the heated polymer due to the accumulation of the oxides produced by thermal degradation of the material on the surface of the volatilizing polymer.^{27,50} This behavior indicates that LDH-CA have great potential for polymer reinforcement.

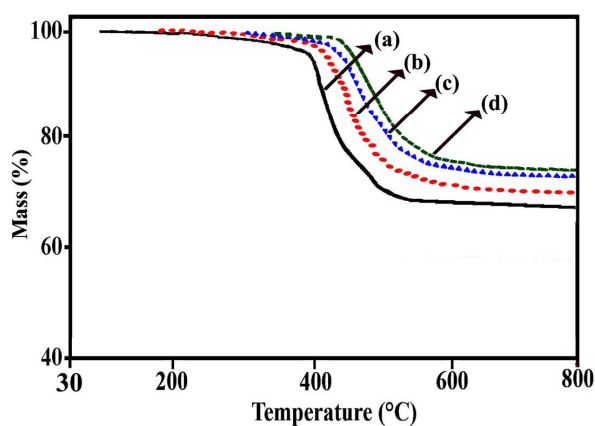


Fig. 8. TGA thermograms of neat PI (a), and NC with 1 (b), 2 (c) and 4wt.% (d) of LDH-CA.

Table 1. Thermal properties of the pure PI and NC with different amount of LDH-CA.

Material	T ₅ (°C) ^a	T ₁₀ (°C) ^a	Char yield (%) ^b
Pure PI	398	407	68
PI/LDH-CA NC1%	423	436	70
PI/LDH-CA NC2%	447	461	73
PI/LDH-CA NC4%	460	486	74

^a Temperature at which 5 and 10% weight loss was recorded by TGA at heating rate of 20 °C min⁻¹ in a N₂ atmosphere.

^b Weight percent of the material left undecomposed after TGA at maximum temperature 800 °C in a N₂ atmosphere.

Conclusions

Herein, a soluble aromatic polyimide containing pendant benzonitrile groups was synthesized by the reaction of 3-(bis(4-aminophenyl)amino)benzonitrile and 4,4'-benzophenone tetracarboxylic dianhydride by thermal imidization method. Layered double hydroxide intercalated with citric acid was prepared through co-precipitation method and polyimide/layered double hydroxide-citric acid nanocomposites were successfully prepared by *in situ* polymerization technique. FT-IR and XRD results show that citrate anions are present in the Zn/Al layered double hydroxide such these materials are layered with large interlayer spaces of 1.98 nm. Morphology, structure and properties of the polyimide/layered double hydroxide-citric acid nanocomposite films were characterized. TEM results showed that the layered double hydroxide-citric acid nanolayers were homogeneously dispersed in polymer matrixes. Dispersed organoclay platelets into polyimide matrix were found to increase the thermal stability such as

thermal decomposition temperature and char yield of polyimide/layered double hydroxide-citric acid nanocomposites. The tensile strength increases with increasing amount of layered double hydroxide-citric acid up to certain content. For the polyimide/layered double hydroxide-citric acid nanocomposites, the maximum degree of tensile strength is observed at a layered double hydroxide-citric acid loading of 2 wt%, corresponding to an almost 32% increase in tensile strength compared to pure polymer. According to the obtained results in this study, by using suitable modifier for layered double hydroxide and in situ polymerization technique, nanocomposites materials with good thermal and mechanical properties could be obtained. These novel high-performance hybrid materials demonstrate a promising potential for future application.

Notes

The authors declare no competing financial interest.

Acknowledgements

We wish to express our gratitude to the Research Affairs Division Isfahan University of Technology (IUT), Isfahan, for partial financial support. Further financial support from National Elite Foundation (NEF), and Iran Nanotechnology Initiative Council (INIC) is gratefully acknowledged.

References

- 1 S. Ghosh, D. Ghosh, P. K. Bag, S. C. Bhattacharya, A. Saha, *Nanoscale*, 2011, **3**, 1139-1148.
- 2 M. Alexandre, P. Dubois, *Mater. Sci. Eng.*, 2000, **28**, 1-63.

- 3 H. Zou, S. Wu, J. Shen, *Chem. Rev.*, 2008, **108**, 3893-3957.
- 4 S. S. Sinha, M. Okamoto, *Prog. Polym. Sci.*, 2003, **28**, 1539-1641.
- 5 M. J. A. Hore, R. J. Composto, *Macromolecules*, 2014, **47**, 875-887.
- 6 M. Garima, D. Vivek, Y. R. Kyong, S. J. Park, W. R. Lee, *J. Ind. Eng. Chem.*, 2015, **21**, 11-25.
- 7 B. Chen, J. R. G. Evans, H. C. Greenwell, A. A. Bowden, A. Whiting, *Chem. Soc. Rev.*, 2008, **37**, 568-594.
- 8 R. J. Sengwa, S. Choudhary, *J. Appl. Polym. Sci.*, 2014, **131**, 40617-40628.
- 9 Y. Yuan, Y. Zhang, W. Shi. *Appl. Clay Sci.*, 2011, **53**, 608-614.
- 10 M. F. Chiang, T. M. Wu. *Compos. Sci. Technol.*, 2010, **70**, 110-115.
- 11 D. Basu, A. Das, K. W. Stockelhuber, U. Wagenknecht, G. Heinrich. *Prog. Polym. Sci.*, 2014, **39**, 594-626.
- 12 Y. C. Li, Y. H. Yang, J. R. Shields, R. D. Davis, *Polymer*, 2015, **56**, 284-292.
- 13 L. Yang, B. Fan, X. Cui, X. Shi, R. Li, *J. Ind. Eng. Chem.*, 2015, **21**, 689-695.
- 14 K. Zargoosh, S. Kondori, M. Dinari, S. Mallakpour, *Ind. Eng. Chem. Res.*, 2015, **54**, 1093-1102.
- 15 B. Hai, Y. Zou, *Sensors Actuators B: Chem.*, 2015, **208**, 143-150.
- 16 Y. Tao, L. Ruiyi, Y. Tingting, L. Zaijun, *Electrochimica Acta*, 2015, **152**, 530-537.
- 17 P. S. Braterman, Z. P. Xu and F. Yarberry, *layered double hydroxides (LDHs)*, in *Handbook of Layered Materials*, eds. S. M. Auerbach, K. A. Carrado and P. K. Dutta, Marcel Dekker, New York, 2004, ch. 8, pp. 373-474.
- 18 P. Roy Chowdhury, K. G. Bhattacharyya, *Dalton Trans.*, 2015, **44**, 6809-6824.
- 19 S. Mallakpour, M. Dinari, A. Nabiyan, *J. Polym. Res.*, 2015, **22**, 11-19.
- 20 J. R. Ebdon, B. Hunt, P. J. Joseph, *Polym. Degrad. Stab.*, 2004, **83**, 181-189.

- 21 S. B. Eshwaran, D. Basu, S. R. Vaikuntam, B. Kutlu, S. Wiessner, A. Das, K. Naskar, G. Heinrich, *J. Appl. Polym. Sci.*, 2015, **132**, 41539-47.
- 22 F. R. Costa, A. Leuteritz, U. Wagenknecht, D. Jehnichen, L. Haußler, G. Heinrich, *Appl. Clay Sci.*, 2007, **38**, 153-164.
- 23 C. Manzi-Nshuti, P. Songtipya, E. Manias, M. del Mar Jimenez-Gasco, J. M. Hossenlopp, C. A. Wilkie, *Polym. Degrad. Stab.*, 2009, **94**, 2042-2054.
- 24 L Qiu, W Chen, B. Qu, *Polym. Degrad. Stab.*, 2005, **87**, 433-440.
- 25 G. Huang, S. Chen, P. Song, P. Lu, C. Wu, H. Liang, *Appl. Clay Sci.*, 2014, **88-89**, 78-85.
- 26 P. Ding, B. Kang, J. Zhang, J. Yang, N. Song, S. Tang, L. Shi, *J. Colloid Interface Sci.*, 2015, **440**, 46-52.
- 27 J. Ahn, M. Han, C. S. Ha, *Polym. Int.*, 2011, **60**, 271-278.
- 28 S. Mallakpour, M. Dinari, M. Hatami, *RSC Adv.*, 2014, **4**, 42114-42121.
- 29 M. S. Cho, B. Shin, J. Do Nam, Y. Lee, K. Song, *Polym. Int.*, 2004, **53**, 1523-1529.
- 30 C. TaviotGueho, F. Leroux, *Struct. Bond.*, 2006, **119**, 121-159.
- 31 I. S. Chung, S. Y. Kim, *Macromolecules*, 1998, **31**, 5920-5923.
- 32 J. Liu, Y. Nakamura, T. Ogura, Y. Shibasaki, S. Ando, M. Ueda, *Chem. Mater.*, 2008, **20**, 273-281.
- 33 M. Dinari, H. Ahmadizadegan, P. Asadi, *New J. Chem.*, 2015, **39**, 4478-4487.
- 34 J. de Abajo, J. G. de la Campa, In: H. R. Kricheldorf, Editor. *Processable aromatic polyimides*, Berlin: Springer; 1999. p. 23-61.
- 35 L. Zhuo, K. Kou, Y. Wang, P. Yao, G. Wu, *J. Mater. Sci.*, 2014, **49**, 5141-5150.
- 36 A. Ghosh, S. K. Sen, S. Banerjee, B. Voit, *RSC Adv.*, 2012, **2**, 5900-5926.
- 37 M. Dinari, H. Ahmadizadegan. *RSC Adv.*, 2015, **5**, 26040-26050.

- 38 M. Dinari, H. Ahmadizadegan, *Polymer*, 2014, **55**, 6252-6260.
- 39 Y. Yuan, Y. Zhang, W. Shi, *Appl. Clay Sci.*, 2011, **53**, 608-614.
- 40 Y. Zhao, F. Li, R. Zhang, D. G. Evans, X. Duan, *Chem. Mater.*, 2002, **14**, 4286-4291.
- 41 S. Mallakpour, M. Dinari, *J. Therm. Anal. Calorim.*, 2013, **114**, 329-337.
- 42 B. Li, J. He, *J. Phys. Chem. C.*, 2008, **112**, 10909-10917.
- 43 N. T. Whilton, P. J. Vickers, S. Mann, *J. Mater. Chem.*, 1997, **7**, 1623-1629.
- 44 K. Zou, H. Zhang, X. Duan, *Chem. Eng. Sci.*, 2007, **62**, 2022-2031.
- 45 F. Barahuie, M. Z. Hussein, S. A. Gani, S. Fakurazi, Z. Zainal, *J. Solid State Chem.*, 2015, **221**, 21-31.
- 46 F. Cavani, F. Trifiro, A. Vaccari, *Catal. Today.*, 1991, **11**, 173-301.
- 47 P. Ding, B. Kang, J. Zhang, J. Yang, N. Song, S. Tang, L. Shi, *J. Colloid Interface Sci.*, 2015, **440**, 46-52.
- 48 E. M. Seftel, E. Popovici, M. Mertens, K. De Witte, G. Van Tendeloo, P. Cool, E. F. Vansant, *Micropor. Mesopor. Mater.*, 2008, **113**, 296-304.
- 49 H. B. Hsueh, C. Y. Chen, *Polymer.*, 2003, **44**, 1151-1161.
- 50 T. Agag, T. Koga, T. Takeichi, *Polymer.*, 2001, **42**, 3399-3408.

In situ thermal synthesis of novel polyimide nanocomposite films containing organo-modified layered double hydroxide: Morphological, thermal and mechanical properties

